Biometric Recognition Based on Hand Electromagnetic Scattering at Microwaves

Emanuele Maiorana, *Senior Member, IEEE*, Davide Ramaccia, *Senior Member, IEEE*, Luca Stefanini, *Graduate Student Member, IEEE*, Alessandro Toscano, *Senior Member, IEEE*, Filiberto Bilotti, *Fellow, IEEE*, and Patrizio Campisi, *Fellow, IEEE*

***Abstract*— In recent years, the need for secure, reliable, and easy-to-use automatic recognition approaches has favored the diffusion of biometric systems. Such methods exploit individuals' physical or behavioral characteristics to differentiate between legitimate users and potential impostors. In this article, we evaluate the feasibility of recognizing a subject by exploiting the electromagnetic (EM) scattering from the user's hand or wrist when it interacts with an EM field at microwave (MW) frequencies. In detail, the proposed recognition framework requires a subject to place a hand between two antennas emitting at frequencies in the *X*-band, i.e., between 8.2 and 12.4 GHz. The measured scattering parameters are employed as discriminative characteristics to perform user recognition. To improve the achievable recognition performance, an EM model of the involved body parts has been studied and used to design a metasurface (MTS) wristband that could emphasize subject-specific characteristics. The effectiveness of the proposed approach has been tested by collecting multiple measurements from 43 subjects during two distinct acquisition sessions. The obtained results testify that the proposed approach can be used either to implement a robust stand-alone biometric system or exploited together with other well-established hand characteristics such as fingerprint, palm print, or hand vein to improve the achievable recognition performance.**

***Index Terms*— Biometric recognition, electromagnetic (EM) metamaterials, hand biometrics, microwave (MW) antennas, passive circuits, scattering parameters, signal processing.**

I. Introduction

BIOMETRIC recognition systems have been studied for more than 50 years [1] to design methods and techniques to automatically recognize a person, by exploiting either physical or behavioral characteristics of the interested subjects. Such systems have been originally developed for forensic applications, such as the identification of possible culprits during investigations, focusing on physical traits such as fingerprint and face [2]. Starting from the 1990s, an increasing interest from both industry and academia has ignited research to design and exploit biometric recognition systems as an alternative to authentication methods relying on the use of passwords or tokens [3].

Biometric systems have some advantages over conventional approaches for user recognition, such as their higher usability. In fact, a biometric trait cannot be lost or forgotten, as it can instead happen for other traditionally used identifiers. Moreover, systems relying on biometric data are commonly considered able to guarantee higher security against potential attacks of malicious subjects, with respect to classical methods, since personal traits are harder to be stolen or acquired without their owners' permission. However, this last consideration is questionable since several biometric features are exposed, such as behavioral traits like signature or gait, or physical traits such as fingerprint, face, or iris. It is in fact well known that malicious subjects can nowadays easily create replicas of some traits with the purpose of violating biometric systems, by covertly capturing traits such as face or iris or recovering latent fingerprints left on some surfaces, and using them as unauthorized identifiers to carry out presentation attacks [4]. In order to implement countermeasures against such spoofing possibilities, the capability of performing liveness detection has become crucial for the design of robust biometric systems [5]. In addition, the study of biometric characteristics that are not exposed, and therefore not easily accessible by attackers, has recently received significant attention [6].

For instance, subcutaneous vein patterns have been extensively investigated, with the main purpose of designing systems robust against spoofing attacks [7]. Vein patterns are usually acquired using near-infrared (NIR) light. At those frequencies, light can penetrate human skin and be absorbed by the hemoglobin in the blood with a higher absorption coefficient compared to water and lipid tissues, with the consequent possibility of allowing to capture images with darker parts in correspondence with the vein vessels. However, NIR-based vein pattern acquisition can be influenced by environmental illumination conditions that could significantly interfere with the acquisition process [8].

As an alternative approach to capture subcutaneous traits in unconstrained environments, still allowing a user-friendly interaction with the acquisition devices, it has been recently proposed to design biometric recognition systems relying on

Manuscript received 20 March 2023; revised 18 May 2023; accepted 17 July 2023. Date of publication 14 August 2023; date of current version 6 November 2023. This work was supported in part by the H2020 Electronics Components and Systems for European Leadership (ECSEL) EU Project "Intelligent Secure Trustable Things" (InSecTT) through the ECSEL Joint Undertaking (JU) under Grant 876038. The document reflects only the author's view, and the Commission is not responsible for any use that may be made of the information it contains. *(Corresponding author: Emanuele Maiorana.)*

The authors are with the Section of Applied Electronics, Department of Industrial, Electronic and Mechanical Engineering, Roma Tre University, 00146 Rome, Italy (e-mail: emanuele.maiorana@uniroma3.it; davide.ramaccia@uniroma3.it; luca.stefanini@uniroma3.it; alessandro.toscano@uniroma3.it; filiberto.bilotti@uniroma3.it; patrizio.campisi@uniroma3.it).

Color versions of one or more figures in this article are available at https://doi.org/10.1109/TMTT.2023.3300175.

Digital Object Identifier 10.1109/TMTT.2023.3300175

the use of radiation with wavelengths longer than those of NIR light, such as those characterizing microwave (MW) frequencies. Following such approach, in addition to performing recognition relying on unexposed traits, thus increasing the inherent security of the biometric system, it is also possible to make the system insensitive to the environmental lighting conditions, which instead could affect NIR-based imaging systems.

While it can be observed that systems relying on MWs may suffer from a loss in resolution with respect to visible and NIR radiation, due to the use of longer wavelengths, it is also worth remarking that this aspect could be in part compensated by the higher penetration depth of the MW radiation, with the collected information being therefore associated with deeper body portions [9]. Furthermore, biological tissues absorb less radiation when lower frequencies are used, thus reducing the tissue heating or discomfort [10]. Therefore, in the last few years, several MW-based recognition systems, making use of different traits of the human body, have been investigated, exploiting frequencies ranging from the sub-GHz regime up to millimeter waves.

In this article, we propose a biometric recognition system relying on the interaction of a user's hand with a broadband electromagnetic (EM) field in the X-band. The main contributions of this work are the following ones.

1) We propose a novel biometric recognition system based on the use of two broadband horn antennas, pointing one toward the other, able to simultaneously radiate and capture the EM field propagating between them. The EM field changes when the user's palm or wrist is placed between the antennas. In fact, the power of the received EM field changes frequency-by-frequency depending on the user's physical characteristics. Biometric data can thus be collected through the two antennas in terms of scattering parameters, thus producing an extremely simple and compact representation of the user's EM properties, which can be employed for user recognition.
2) We propose a novel applicative scenario of flexible metasurfaces (MTSs), which is used here to emphasize subject-specific EM scattering characteristics when wrapped around the users' wrist. In more detail, the MTS unit cells (UCs) operate in two subbands characterized by a higher reflection of the EM field, and an additional subband characterized by a stronger absorption than the user's wrist alone.
3) The techniques employed to process the captured EM scattering parameters are specifically designed to make the proposed system suitable for biometric verification scenarios, that is, for conditions typically considered in access control applications, where individuals have to be recognized in order to gain access to restricted physical or logical environments or resources.

Fig. 1 shows a possible operative access control scenario, where the proposed MW-based system is employed to grant access to a reserved area. Two antennas integrated in the biometric system on the door radiate and simultaneously capture the MW field. The scattering profile of the user is compared with the stored one, granting access when the user is recognized. It is worth remarking that, since the proposed system relies on the EM scattering properties of a user's palm or wrist, by design, it can be easily integrated with recognition systems based on fingerprint, palm print, or hand vein patterns, realizing a multibiometric system. Within a multibiometric system, the considered MW-based biometric identifiers could be exploited both to improve the achievable recognition rates as well as to increase the overall system robustness against spoofing attacks.

Fig. 1. Representation of an access control application with a device mockup of the proposed MW-based biometric recognition system and the exploitation of the designed MTS wristband.

This article is organized as follows. Section II provides a brief survey about the exploitation of MW radiation for biometric recognition purposes. A detailed description of the proposed biometric recognition system is outlined in Section III, together with the approaches employed to acquire and process the considered signals. Section IV is focused on the modeling and design of the unit cell used to realize the flexible MTS wristband. The tests performed and the experimental results obtained are then detailed in Section V, while conclusions are finally drawn in Section VI.

II. MW Fields for Biometric Recognition: State-of-the-Art

In the last decade, the use of EM fields at MW frequencies for biometric recognition has attracted significant interest in the scientific community due to the strong interaction that they may have with the human body or parts of it, given the comparable dimensions of some traits of the human body, such as head, hands, and arms, and the MW free-space operative wavelengths (from 1 mm to 1 m) [10].

In this scenario, the first attempts have exploited radar systems, relying on the Doppler effect to derive discriminative information related to specific movements of a person. For instance, heart-induced movements of the chest cage have been considered to design contactless recognition systems in [11] and [12]. When focusing on lower frequencies of the signals received by radar, it is also possible to recover information on the respiratory activity of the subject and use this information to recognize people [13]. Large-scale movements associated with the gait of a person have also been analyzed using radars and exploited to perform biometric recognition as in [14].

TABLE I
STATE-OF-THE-ART ON THE USE OF MWS FOR BIOMETRIC RECOGNITION PURPOSES

Approach	Trait	Reference	Subjects	Frequency	Classifier	Performance	
						R1	EER
Radar	Heart	[11]	26	2.4 GHz	*k*-NN	14.4%	-
		[12]	11	24 GHz	L2 distance	-	3.9%
	Breath	[13]	5	2.4 GHz	*k*-NN	92.0%	-
	Gait	[14]	18	77 GHz	Neural network	76.2%	-
WiFi	Body	[15]	11	5.9 GHz	Cosine	98.8%	-
		[16]	30	5 GHz	SVM	92.0%	-
	Breath	[17]	20	5 GHz	L2 distance	-	10.8%
		[18]	24	5 GHz	GMM	-	5.0%
	Gait	[19]	24	5 GHz	Neural network	87.7%	-
		[20]	50	5 GHz	Neural network	99.7%	-
	Posture	[21]	30	5 GHz	Autoencoder	-	1.8%
	Keystroke	[22]	9	5 GHz	*k*-NN	85.2%	-
RFID	Finger	[23]	15	922 MHz	SVM	-	5.0%
	Hand	[24]	30	920 MHz	Neural network	99.0%	-
Wearable	Arm	[25]	50	2.4 GHz	MLP	98.6%	-
		[26]	6	2.4 GHz	MLP	98.0%	-
Imaging	Hand	[28]	37	9.6 GHz	Polynomial	94.7%	-
	Face	[29]	200	60 GHz	Autoencoder	-	1.0%
Scattering	Finger	[27]	5	57–64 GHz	Random forest	98.0%	-
	Hand	[30]	3	900 MHz–2.4 GHz	n/a	-	-
		[31]	8	8.2–12.4 GHz	L1 distance	-	8.0%

The same methodology has also been applied in the case of opportunistic illuminators, such as Wi-Fi devices, whose channel state information (CSI) has been used to perform people recognition across walls [15]. This modality typically requires the involved subjects to be still in a standing or sitting posture during data collection [16], [17], [18]. Nonetheless, the CSI has also been employed to derive discriminative information associated with walking subjects, through the analysis of the time-varying characteristics of the monitored Wi-Fi channel [19], [20]. Subject-specific patterns associated with other activities, such as postural transitions [21] or keyboard typing [22], have also been analyzed through contactless acquisition modalities relying on Wi-Fi signals. It is worth mentioning that all the aforementioned systems make use of only behavioral traits, modeling the user simply as a highly reflective scatterer.

When an EM field interacts with the biological tissue, the body composition and shape play an important role in the interaction process, which is different from subject to subject according to the amount of water, fat, skin conditions, size, and other biological features. To exploit this kind of interaction, passive radio frequency identification (RFID) tags have been recently considered in [23] and [24]. Biometric identifiers have been derived by measuring the backscattered signal obtained when placing a finger over RFID tags, whose frequency response is directly affected by the effective relative permittivity and conductivity of a user's finger. Active antennas have been employed in [25] and [26], realizing a recognition system based on the transmitted signal generated by two wearable antennas on the user's arm, whereas in [27] four transmitting and two receiving antennas have been used to collect subject-specific information when four fingers of a hand are placed over them. However, all the mentioned methods are not suitable in contactless scenarios since direct contact with the measuring system is always needed. Contactless MW-based recognition systems have been proposed in [28] and [29], yet the needed acquisition time is not compatible with applications requiring fast recognition times. A contactless system based on a single antenna has been recently proposed in [30] and [31], exploiting the input impedance matching level and the backscattering level, respectively, to perform user recognition.

A summary of the state-of-the-art on the use of MW radiation for biometric recognition purposes is reported in Table I. For each considered work, the table reports the operative frequency range, the number of subjects involved in the performed tests, the achieved recognition performance, expressed in terms of rank-1 (R1) accuracy for identification systems, and equal error rate (EER) for systems working in the verification modality. Most of the performed studies have been carried out considering identification scenarios, where it is assumed to have knowledge about the characteristics of all the users involved in the recognition process when training the employed classifiers. The recognition rates estimated in this modality are highly dependent on the number of considered users, which typically assumes low values in the performed studies. Moreover, such scenarios are typically employed for surveillance purposes, which can be hardly managed through the proposed MW-based technologies, which are conversely more suited for access control applications.

The contribution here presented stems from the one in [31] and evaluates the feasibility of performing biometric verification relying on the EM interaction of a user's hand with the field radiated by a set of two MW antennas, instead of a single one as in [31]. The proposed system has been designed

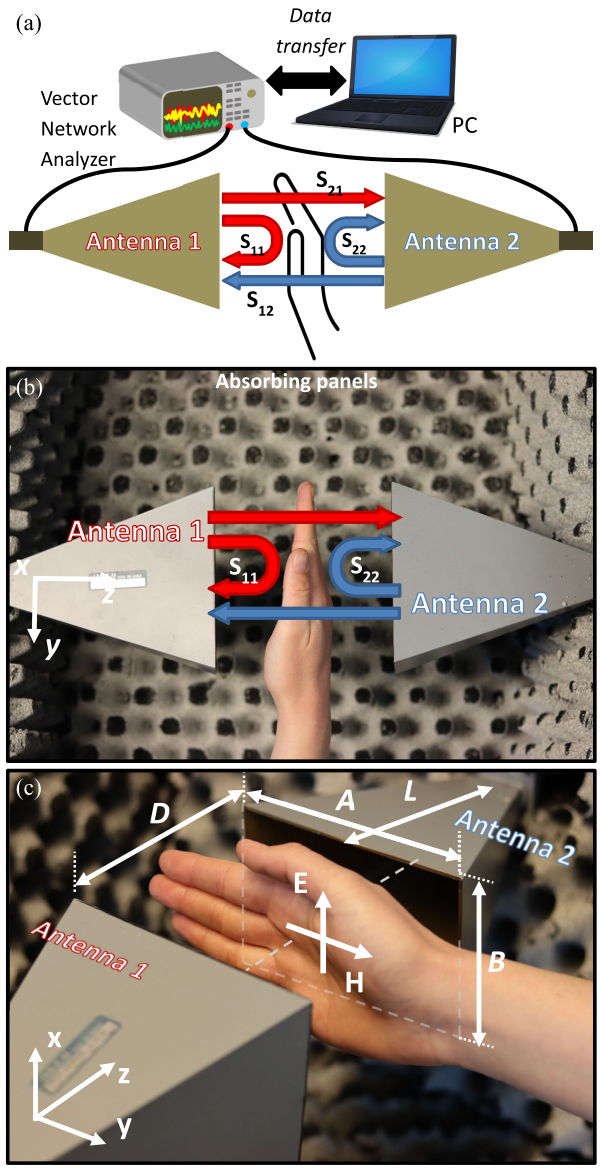

Fig. 2. Proposed MW-based recognition system. (a) Schematic of the entire system, (b) picture (top view) of the antennas with user hand, and (c) picture (perspective view) of the antennas with dimensions of the antenna apertures and distance between them.

to guarantee a seamless and swift interaction with the users to be authenticated.

III. Proposed MW-Based Biometric Recognition System

In this section, we describe the proposed recognition system integrating an acquisition setup, two MW horn antennas, and a vector network analyzer (VNA) connected to a computer for the processing of the acquired data. In more detail, a description of the framework employed to collect the EM response and the corresponding data is provided in Section III-A, whereas the processing performed on the collected data to perform biometric recognition is detailed in Section III-B.

A. MW Acquisition System

The proposed acquisition system is shown in Fig. 2. It consists of two horn antennas, each of them fed by a WR90 rectangular waveguide supporting monomodal propagation in the frequency range 8.2–12.4 GHz, i.e., in the MW X-band. The EM field is linearly polarized, with the electric field vector oscillating along the x-direction and magnetic field along the y-direction, as shown in Fig. 2(c). Within this frequency range, the free-space wavelengths range from about 24 mm (at 12.4 GHz) to 36 mm (at 8.2 GHz), making them fully comparable with the average feature dimensions of hands and wrist. The dimensions of the horn antennas, as reported in Fig. 2(c), are: aperture width $A = 145$ mm, aperture height $B = 100$ mm, and horn length $L = 175$ mm. The dimensions ensure an antenna gain greater than 20 dBi in their respective broadside direction, i.e., positive z-direction for Antenna 1 and negative z-direction for Antenna 2, in the entire operative band. As shown in Fig. 2(b) and (c), the antennas are aligned along the z-axis, and their apertures are placed at a distance $D = 100$ mm from each other, realizing a free-space volume of $V = 1.45$ dm^3, where the user can insert a hand for biometric characterization (see Fig. 2(c)).

The antennas are connected to a two-port VNA via a pair of coaxial cables for signals up to 18 GHz and terminated by SMA connectors. The VNA is a Rohde and Schwarz ZVB 14, operating from 100 MHz up to 14 GHz, able to measure all the complex scattering parameters at the ports connected to the antennas. In more detail, as shown in Fig. 2(a) and (b), the VNA measures and records the complex scattering parameters S_{11} and S_{22} in reflection and S_{12} and S_{21} in transmission [32]. Before the acquisition campaign, the antenna system has been calibrated via thru-short-match (TSM) method [33], to have unitary transmission and zero reflection recorded by the VNA when the user is not present.

The modality of interaction with the EM field radiated by the antennas requires that the user places the palm or wrist in the volume between the two antennas as shown in Fig. 2(c). As shown in Fig. 2(b) and (c), in the performed tests, the acquisitions have been made with an outstretched hand, fingers together, when collecting the scattering parameters associated with both palm and wrist. While the employed fingers posture is a requirement to take consistent acquisitions for traits associated with the palm, it is not relevant for acquisitions related to the wrist.

The VNA measures the full set of complex scattering parameters, which contain information associated with the EM characteristics of the user hand traits. Being complex, each of the employed biometric identifiers S_{11}, S_{21}, S_{12}, and S_{22} is expressed in terms of an amplitude–phase pair as functions of frequency.

Finally, as shown in Fig. 2(a), all collected data are transferred to the personal computer for the processing and user identification steps. The applied signal processing and the employed recognition algorithms are described in Section III-B.

B. Signal Processing for Biometric Recognition

The scattering parameters, measured during each interaction of a user with the proposed system, are employed as biometric identifiers upon which a verification process can be carried out.

Specifically, it is assumed that a user provides E samples of the considered biometric traits during an enrolment stage. The acquisitions collected during the registration of a subject can be thus generically represented as a set $\boldsymbol{s}_r^{(e)}, e = 1, \ldots, E$, where each vector $\boldsymbol{s}_r^{(e)} \in \mathbb{R}^F$ has a length F depending on the considered frequency range and resolution, on which scattering parameters are considered as biometric identifiers, and on the representation of the employed parameters, which can be expressed in terms of amplitude, phase, or both.

When a probe sample $\boldsymbol{s}_v$ is collected during a verification stage, it is compared against the samples collected from the user whose identity has been claimed, in order to determine whether the presented subject is an impostor or not. Typically, a similarity (or dissimilarity) score between the probe sample and the enrolment set is computed, and a decision is taken by comparing the obtained score against a threshold. The required (dis)similarity score can be computed by considering only the information provided by the legitimate user during the enrolment, as outlined in Section III-B1. Alternatively, information gathered from a set of subjects can also be employed to model the characteristics of potential impostors and exploited to compute the needed score, as detailed in Section III-B2.

1) Similarity Scores Based on Genuine Data Only: Several metrics can be employed to evaluate the similarity between a sample and a set of reference patterns. In the performed tests, we have considered the following ones.

1) A dissimilarity score can be computed as the minimum among the Manhattan (L1) distances between the probe and each of the E enrolment samples as follows:

$$D_{L1} = \min_e \left\{ \sum_{f=1}^{F} \boldsymbol{d}_{L1}^{(e)}[f] \right\}$$
$$\boldsymbol{d}_{L1}^{(e)}[f] = \left| \boldsymbol{s}_v[f] - \boldsymbol{s}_r^{(e)}[f] \right|. \tag{1}$$

2) In order to consider the differences in intraclass variability of different scattering parameters and distinct frequency ranges, normalized distances between probe and enrolment samples can be computed as follows:

$$D_{L1z} = \min_e \left\{ \sum_{f=1}^{F} \boldsymbol{d}_{L1z}^{(e)}[f] \right\}$$
$$\boldsymbol{d}_{L1z}^{(e)}[f] = \frac{\left| \boldsymbol{s}_v[f] - \boldsymbol{s}_r^{(e)}[f] \right|}{\boldsymbol{s}[f]} \tag{2}$$

with $\boldsymbol{s}[f]$ representing the standard deviation of the fth coefficient, computed over the E samples collected during the enrolment of the considered user.

3) In order to further normalize the behavior exhibited by different contributions in the employed identifiers, another dissimilarity measure can be defined by simply counting the number of coefficients for which the considered probe is distant from the corresponding mean by a given number of standard deviations, i.e.,

$$\begin{cases} D_T = \sum_{f=1}^{F} \boldsymbol{p}[f] \\ \boldsymbol{p}[f] = 1, \quad \text{if } \dfrac{\left| \boldsymbol{s}_v[f] - \boldsymbol{m}[f] \right|}{\boldsymbol{s}[f]} > T \\ \boldsymbol{p}[f] = 0, \quad \text{otherwise} \end{cases} \tag{3}$$

being $\boldsymbol{m}[f]$ the mean of the fth coefficient for the considered user and T the employed threshold.

4) A one-class support vector machine (OC-SVM) can be trained using the E samples collected during the user's enrolment, thus using data from a single class for training purposes. In the performed tests, a Gaussian kernel is employed to train the considered models. When a probe sample is submitted during the verification stage, a similarity measure can be computed using the trained model and, if necessary, inverted to provide a dissimilarity score $D_{\text{OC-SVM}}$.

It is worth remarking that, in addition to the mentioned measures based on L1 distance, analogous metrics relying on Euclidean (L2), cosine, and Mahalanobis distances have been considered in the performed tests. Nonetheless, due to the worst results obtained with their use, these additional measures are not considered in the following discussion.

2) Similarity Scores Based on Potential Impostor Data: In order to gather information regarding which contributions in the employed identifiers should be given more consideration to carry out the recognition process effectively, it can be assumed that, during the enrolment of a user, data collected from other subjects are also available and employed to model the characteristics of potential impostors. Having represented the set of data employed to model impostors through the samples $\boldsymbol{s}_w^{(i)}, i = 1, \ldots, I$, the metrics presented in Section III-B1 could be modified in order to consider such additional knowledge as follows.

1) A corrective factor for L1 distances can be computed as follows:

$$\boldsymbol{c}_{L1}[f] = \frac{1}{I} \sum_{i=1}^{I} \min_e \left\{ \left| \boldsymbol{s}_w^{(i)}[f] - \boldsymbol{s}_r^{(e)}[f] \right| \right\} \tag{4}$$

and a dissimilarity measure emphasizing the contributions that are expected to be more specific to the enrolled user can be then computed as follows:

$$D_{L1}^{\text{IMP}} = \min_e \left\{ \sum_{f=1}^{F} \boldsymbol{d}_{L1}^{(e)}[f] \times \boldsymbol{c}_{L1}[f] \right\}. \tag{5}$$

2) Similar to the previous case, in order to emphasize the contributions exhibiting the greatest differences between genuine and impostor samples, a corrective factor can be computed as follows:

$$\boldsymbol{c}_{L1z}[f] = \frac{1}{I} \sum_{i=1}^{I} \min_e \left\{ \frac{\left| \boldsymbol{s}_w^{(i)}[f] - \boldsymbol{s}_r^{(e)}[f] \right|}{\boldsymbol{s}[f]} \right\} \tag{6}$$

and employed to evaluate the dissimilarity score

$$D_{L1z}^{\mathrm{IMP}} = \min_{e} \left\{ \sum_{f=1}^{F} \boldsymbol{d}_{L1z}^{(e)}[f] \times \boldsymbol{c}_{L1z}[f] \right\}. \tag{7}$$

3) A corrective factor considering samples modeling impostors' behavior can also be computed as follows:

$$\begin{cases} \boldsymbol{c}_T[f] = \dfrac{1}{I} \displaystyle\sum_{i=1}^{I} \boldsymbol{p}_w^{(i)}[f] \\ \boldsymbol{p}_w^{(i)}[f] = 1, \quad \text{if } \dfrac{\left| \boldsymbol{s}_w^{(i)}[f] - \boldsymbol{m}[f] \right|}{\boldsymbol{s}[f]} > T \\ \boldsymbol{p}_w^{(i)}[f] = 0, \quad \text{otherwise} \end{cases} \tag{8}$$

in order to evaluate the dissimilar distance

$$D_T^{\mathrm{IMP}} = \sum_{f=1}^{F} \boldsymbol{p}[f] \times \boldsymbol{c}_T[f]. \tag{9}$$

4) A binary SVM can be trained with a class represented by the E samples collected during the user's enrolment, and the other one described through the I samples employed to model impostors' characteristics. The trained model is used during verification to compute a dissimilarity score D_{SVM} when a probe sample is collected.
5) Classification trees have also been considered in the performed tests, relying on a random forest (RF) approach, i.e., using ensembles of classification trees performing random predictor selections at each split of the tree growth. As for binary SVM, the E samples collected during the user's enrolment are used, together with I samples taken to model impostors' characteristics, to train the ensemble. A dissimilarity score D_{RF} is produced at the verification stage as percentage of trees suggesting the impostors' class for the provided probe.
6) Eventually, also the effectiveness of dictionary learning has been investigated. In more detail, techniques belonging to this category look for sparse representations of the input data by linearly combining the coefficients of the original representations, and achieving sparsity using dictionary atoms lying in a space whose dimensionality is greater than the one of the original input. Sparse-representation-based classification (SRC) [34] has been considered in the performed tests, with the associated dissimilarity score indicated in the following as D_{SRC}.

IV. MTS Wristband

In this section, the design of an MTS wristband is presented and discussed. The interaction between the human body and the EM field is a complex phenomenon, involving both backward and forward scattering that define the signature of each user. Even though such processes are well observed when the operative wavelength is comparable with the trait under test, i.e., palm and wrist in this case, the penetration depth of the illuminating EM field is not enough to interact in a significant manner with the innermost biometric characteristics, leading to a loss of information. Therefore, we design an MTS wristband whose functionality is to enhance the scattering and absorption signature of each user, in order to improve the achievable recognition performance.

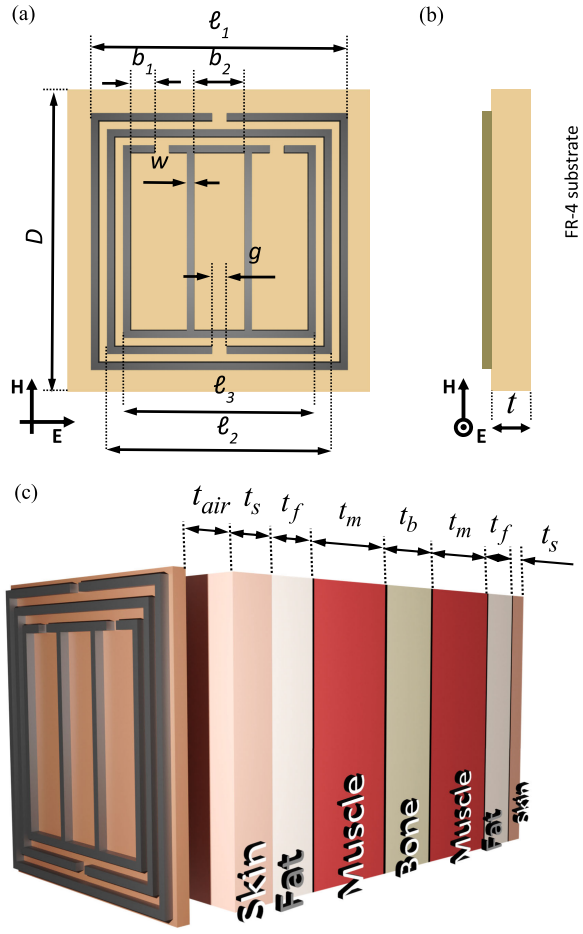

Fig. 3. Graphical representation of (a) front view and (b) side view of the MTS unit cell with dimensions: $D = 8$ mm, $\ell_1 = 6.75$ mm, $\ell_2 = 5.90$ mm, $\ell_3 = 5.07$ mm, $b_1 = 0.68$ mm, $b_2 = 1.38$ mm, $w = 0.15$ mm, $g = 0.38$ mm, and $t = 0.4$ mm. (c) Stack-up of biological tissues (skin, fat, muscles, and bones) for a generic wrist with the proposed MTS UC placed on top.

An MTS is a planar alignment of artificial inclusions, also named meta-atoms, properly engineered in order to exhibit a desired frequency response and/or functionality when interacting with an EM field [35], [36]. In the last decade, MTSs have found application in a huge number of different fields, spanning from telecommunication [37], [38], [39] and radar [40] to photonic devices [41], [42] and sensing [43]. Here, we leverage on the environmental-dependent EM response of the artificial metallic inclusions composing the MTS wristband. In more detail, we introduce a flexible MTS to be wrapped around the user's wrist for emphasizing subject-specific EM scattering and absorption characteristics.

In the following, we describe in detail the selected UC composing the MTS wristband, and the corresponding full-wave numerical simulations performed for characterizing it in the presence of the biological tissue. Then, the designed wristband has been fabricated and used in the recognition system as illustrated in Section V.

A. MTS Unit Cell: Design and Performances

In Fig. 3(a), we report the MTS's UC considered in this work. The UC has square symmetry, and its dimension D

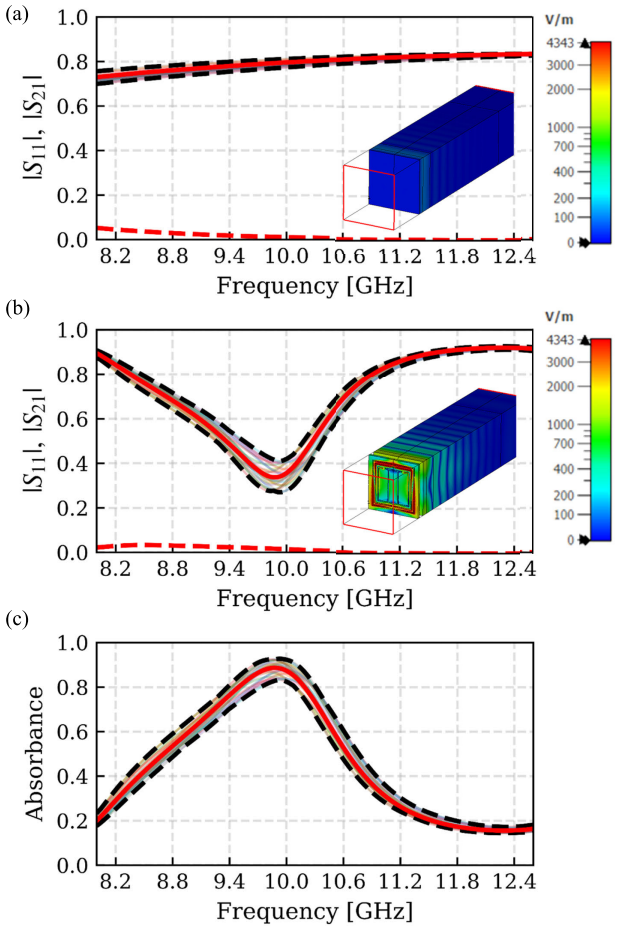

Fig. 4. Parametric study of virtual users. (a) Body stack is simulated without the MSRR and the thickness of the different components is randomly varied between 10% of the nominal value. (b) and (c) Body stack is simulated with the addition of the MSRR and the same virtual user procedure is performed. The variability between different users is clearly enhanced by the resonance of the MSRR. The absorbance peak indicates a strong interaction between the body tissues and the MTS UC.

defines the periodicity of the MTS. Within each UC, a metallic inclusion composed of three concentric square loops is placed at the center of the cell. The sides of the three squares are indicated as ℓ_1–ℓ_3, and the thickness of the metallic strips is w. All of them present some gaps of dimension g, as shown in Fig. 3(a). Finally, two vertical metallic strips connect the opposite sides of the inner square. The UC is designed to respond to an electric field orthogonal to the aforementioned strips on the inner square, TM polarization, as indicated in Fig. 3(a). The inclusion is printed on an electrically thin dielectric substrate of thickness $t = 0.4$ mm and made of FR-4 with relative permittivity $\varepsilon_r = 4.3$ and $\tan\delta = 0.025$ at 10 GHz. The thickness of metallic layer is 18 μm. The proposed UC is also known as a multiple split-ring resonator (MSRR) [44], and it is inspired by the MSRR recently proposed in [45]. All dimensions in millimeters are reported in the caption of Fig. 3.

In order to determine the dimensions of the MTS inclusion as well as the periodicity D, we must consider the interaction with the biological tissues. In Fig. 3(c), we report a graphical representation of the considered stack-up of different tissues composing the transversal section of a human wrist or hand.

TABLE II
ELECTRIC CHARACTERISTICS OF TISSUES AT 10 GHz

Tissue	Relative Permittivity	Conductivity (S/m)	Thickness (mm)
Skin (Dry)	31	8.01	1
Fat	8.80	1.71	2
Muscle	42.8	10.6	20
Bone (Cortical)	8.12	2.14	8

The stack-up is composed of seven layers comprising skin, fat, muscle, and bone in the proper order. From the EM point of view, each tissue is characterized using its relative permittivity ε_r and conductivity σ. The values for each tissue have been extracted from the open database of *Foundation for Research on Information Technologies in Society* [46] and listed in Table II. Moreover, in Table II, the common thicknesses of each tissue in millimeters are reported [47], [48]. The total width of the wrist is around 50 mm, which is fully compatible with the average thickness of an adult. It is worth noticing that a tiny air gap $t_{\text{air}} = 2$ mm is considered between the MTS inclusion and the skin to model the imperfect adherence of the wristband to the skin when worn.

A proper set of full-wave numerical simulations of the structure in Fig. 3(c) is performed in CST MW Studio [49], deriving the optimal dimensions of the MTS's UC and the periodicity to operate in the X-band. The numerical design is carried out by imposing periodic boundary conditions along the transversal directions to replicate the single element in a periodic array as if it were embedded in a realistic MTS. The final dimensions are listed in the caption of Fig. 3.

In Fig. 4(a), we report the numerically computed amplitude of the scattering parameters S_{11} and S_{21} when a TM plane wave illuminates the biological tissue stack-up *without* the designed MTS inclusion in front of it. Due to the symmetry of the stack-up, the other pair of scattering parameters obtained illuminating from the opposite side, i.e., S_{22} and S_{12}, are identical to the reported ones and thus omitted. Fig. 4(a) shows that S_{11} exhibits quite high values and almost flat response (red solid line, Fig. 4(a)), due to strong reflection at the air–skin interface caused by the high permittivity of the tissues (Table II). The (little) amount of EM field that penetrates in the stack-up is absorbed due to the electric losses identified by the conductivity, and therefore, the scattering parameter S_{21} (red dashed line, Fig. 4(a)) is almost zero. This is also graphically shown in the inset of Fig. 4(a), where the numerically computed electric field map at 10 GHz is reported. Moreover, we performed a study varying all thicknesses of the stack-up randomly of $\pm 10\%$, with the aim to determine whether different "virtual" users may exhibit different scattering responses. We conclude that the strong reflection at the air–skin interface does not allow to appreciate a strong variability, as marked by the two dashed black lines in Fig. 4(a). Although the EM signatures of the synthetic users

can be in principle discriminated, their differences are not so pronounced to allow a biometric recognition system to be robust and reliable.

In Fig. 4(b) we report the numerically computed amplitude of the scattering parameters S_{11} and S_{21} of the stack-up when the MTS inclusion is present in front of it. The other pair of scattering parameters, S_{22} and S_{12}, are measured from the naked stack-up side, and hence, they are equal to the ones reported in Fig. 4(a) and neglected. In this case, the presence of the UC significantly alters the in-band scattering response (red solid line, Fig. 4(b)). In particular, the reflection at the edge of the X-band is higher than the case without the UC, whereas at the center of the band (around 10 GHz), a significant reduction of the reflection is achieved. The amount of the EM field passing through the entire stack-up is still extremely low (red dashed line, Fig. 4(b)), due to the losses of tissues. It is worth noticing that the EM field penetrates more in the body, as shown in the inset of Fig. 4(b). This leads to a high energy absorption, quantified in terms of the absorbance quantity $A = 1 - |S_{11}|^2 - |S_{21}|^2$ (Fig. 4(c)), where a strong absorbing behavior is observed around 10 GHz. Finally, a study varying randomly all thicknesses of the stack-up of $\pm 10\%$ is performed. In this case, it is possible to note that the differences among the EM signatures of the virtual users are more pronounced, especially around the maximum absorption frequency, making these results encouraging for establishing a reliable and robust biometric recognition system.

B. Fabrication and Use of the MTS Wristband

In Fig. 5(a), we report a graphical picture of the MTS used for realizing the wristband composed of 40 UCs arranged in a planar array with five rows and eight columns. The overall MTS dimensions are: $L_w = 7.5$ cm and $H_w = 4.8$ cm. The fabrication has been realized by using the printed circuit board (PCB) fabrication technology, based on laser structuring of the copper clad. In particular, the proposed wristband has been realized by using the fast tabletop system LPKF ProtoLaser H4 [50], able to structure the copper of a PCB substrate at the speed of 8.5 cm^2/min, and with an accuracy of ± 5 μm. In Fig. 5(b), we report a photograph of the fabricated wristband at the end of the fabrication process. The metallic inclusions composing the MTS are well-realized and ready for being worn by a user, as shown in Fig. 5(c). Finally, in Fig. 5(d), we report a picture of a user's hand with the fabricated wristband during the acquisition process. The wrist is within the measured volume between the two antennas as described in Section III-A.

V. Experimental Results

An extensive set of experimental tests has been carried out to evaluate the effectiveness of the proposed biometric recognition approach based on the EM interaction of a user's hand with a system composed of a pair of MW antennas. The tests described in the following have been performed using data collected from 43 subjects (18 females and 25 males) during two distinct acquisition sessions taken in distinct days, to consider the possible intraclass variability that could characterize identifiers collected in different occasions. For the considered scenario, each user has interacted with the proposed system ten times during each acquisition session. To ensure that the acquisition conditions are always consistent with the configuration of the proposed system, data corresponding to the right hand have been collected for each involved user.

A. Influence of the Selected Dissimilarity Distance

The influence of the used comparison strategy on the achievable recognition performance has been first evaluated. To this aim, we have staged a scenario in which each of the involved users interacts with the system by placing the used hand between the employed antennas while changing each time the relative distance from them, to simulate a completely free operative condition. Measurements have been taken when both palms and wrists have been placed between the antennas.

Half of the samples collected from each user have been employed for enrolment purposes ($E = 10$), with the remaining ones employed as verification probes to estimate the attainable false recognition rate (FRR). When required, one sample from each of 20 subjects other than the enrolled one has been employed to model the characteristics of potential impostors when exploiting the metrics introduced in Section III-B2 ($I = 20$). Samples from the remaining 22 subjects have been instead considered as verification probes to estimate the system false rejection rate (FAR), thus simulating open-set conditions in the performed tests. The selection of both the employed samples and the subjects used for the impostor's model has been performed randomly for ten different times when computing the achievable performance measures, reported in the following in terms of average over the performed iterations with associated 95% confidence interval.

The used representations $\boldsymbol{s}$ are obtained by considering all the collected scattering parameters S_{11}, S_{12}, and S_{22} (excluding S_{21} to avoid redundancy), each of them expressed in terms of amplitude and phase, over the entire frequency range 8.2–12.4 GHz, scanned with a resolution of 20 MHz, being therefore $F = 1206$.

Table III shows the EERs, i.e., the error corresponding to the system configuration for which FRR and FAR are equal, obtained when using the dissimilarity measures described in Sections III-B1 and III-B2. The parameter T employed for the distances D_T and D_T^{IMP} has been set to $T = 3$ in the performed tests. As can be seen, modeling the behavior of potential impostors by exploiting data collected from a training set of subjects can significantly help improving the achievable recognition rates. Similar results have been obtained when considering either palms or wrists as employed biometric trait. Nonetheless, the achieved recognition rates are quite high, thus highlighting the need for an in-depth study regarding the characteristics to be used and the acquisition conditions to be adopted.

B. Influence of the Employed Scattering Parameters

To evaluate which representation should be applied to define an identifier based on the measured scattering parameters,

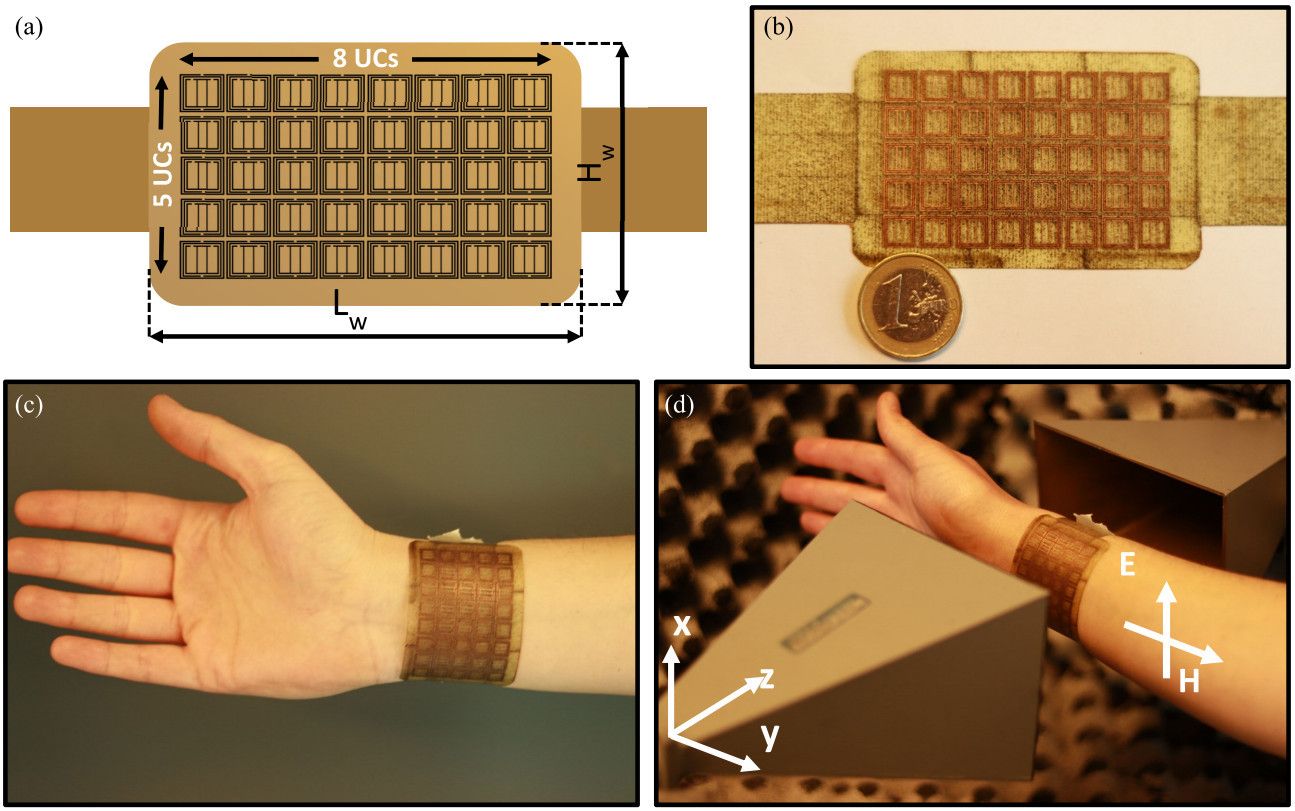

Fig. 5. Proposed MTS wristband. (a) Graphical picture with dimensions, (b) photograph (top view) of fabricated device, (c) photograph (front view) of the wristband worn on right wrist of the user, and (d) photograph (perspective view) of the user with wristband during the acquisition/identification process using the proposed MW biometric system.

TABLE III
MEAN EERS WITH CONFIDENCE INTERVALS (IN %) ACHIEVED IN FREE OPERATIVE CONDITIONS FOR DIFFERENT DISSIMILARITY MEASURES

Trait	Measure									
	D_{L1}	D_{L1z}	D_T	D_{OC-SVM}	D_{L1}^{IMP}	D_{L1z}^{IMP}	$D_T{}^{IMP}$	D_{SVM}	D_{RF}	D_{SRC}
Palm	21.5±0.5	12.8±0.9	13.1±0.7	14.2±0.8	20.1±0.8	12.1±0.8	12.0±0.8	12.9±0.8	12.6±0.8	13.9±0.7
Wrist	20.6±0.7	13.2±0.7	11.7±1.0	13.2±0.8	19.6±0.9	12.5±0.9	9.9±1.0	12.1±0.6	10.7±0.7	14.0±1.1

we have performed tests relying on templates $\boldsymbol{s}$ obtained by considering different scenarios:

1) all the collected information ($F = 1206$);
2) only the amplitude or phase of the collected parameters ($F = 603$);
3) only the amplitude of each individual scattering parameter S_{11}, S_{12}, or S_{22} ($F = 301$).

We have also evaluated whether keeping approximately the same distance from the employed antennas, when placing the hand between them, can improve the achievable performance. Acquisitions have been therefore taken in bound conditions by considering, for both palms and wrists, measurements with hands placed to the side of a foam spacer having a thickness of 30 mm, positioned in front of the left antenna aperture and used as a reference plane.

Furthermore, in order to improve the achievable performance, we perform comparisons using altogether the four best dissimilarity measures, that is, $D_{\mathrm{L1z}}^{\mathrm{IMP}}$, D_T^{IMP}, D_{SVM}, and D_{RF}, as shown by the results in Table III, by carrying out the recognition process based on the sum of the four computed distances.

The results obtained by following the same settings illustrated in Section V-A are given in Table IV for all the considered scenarios. It is possible to observe that jointly exploiting the proposed distances with a score-level information fusion, thus using discriminative characteristics highlighted through different kinds of processing, allows to notably improve the achievable recognition rates. Moreover, asking the involved users to have limited variability in the positioning of the employed biometric trait allows to further enhance the obtained performance. Eventually, the reported results show that most of the discriminative capability of the measured scattering parameters lies in their amplitude, with the phase of the measured characteristics that should be discarded in order to achieve better recognition rates.

C. Influence of the Proposed MTM-Based Wristband

The results shown in Table IV testify that the proposed approach relying on the EM interaction between a user's hand and a pair of MW antennas could guarantee interesting performance, and can be therefore employed to design a biometric recognition system that could be robust against spoofing attack. Nonetheless, in order to reasonably use the proposed biometric characteristics in a real-world scenario, it is desirable to further improve the recognition performance.

TABLE IV
MEAN EERS WITH CONFIDENCE INTERVALS (IN %) ACHIEVED IN FREE AND BOUND CONDITIONS USING DIFFERENT SCATTERING PARAMETERS

Trait	Position	Employed Scattering Parameters					
		All	Amplitude	Phase	S_{11} Amplitude	S_{12} Amplitude	S_{22} Amplitude
Palm	Free	9.8±0.4	9.2±0.5	16.5±1.1	13.9±0.5	13.5±1.2	13.4±0.5
	Bound	8.7±0.7	7.4±0.6	13.0±1.0	11.0±0.5	10.7±0.6	8.6±0.6
Wrist	Free	9.4±0.7	9.3±0.6	14.8±1.0	13.7±0.5	11.7±0.8	12.4±0.8
	Bound	7.2±0.7	6.5±0.4	12.3±0.9	8.5±0.8	9.1±0.8	9.2±0.6

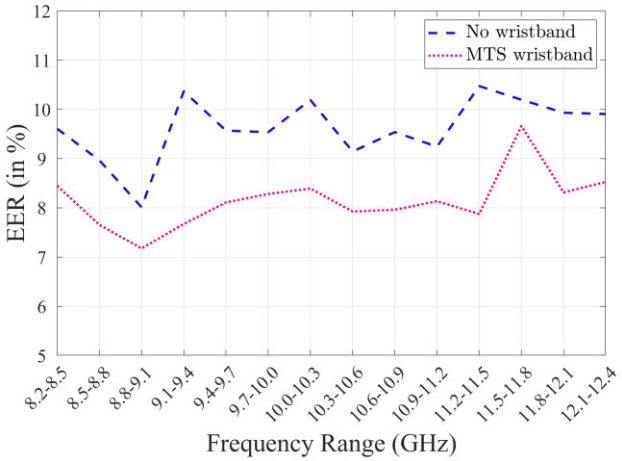

Fig. 6. Recognition performance, in terms of mean EER, achieved using the amplitude of the considered scattering parameters over different frequency ranges as biometric identifier (representations with $F = 45$ coefficients), and an ensemble of the best classifiers.

To this aim, we have evaluated the effectiveness of using the MTS wristband described in Section IV to emphasize subject-specific properties when carrying out a recognition process. Additional acquisitions have been taken from the considered 43 subjects while wearing the proposed MTS wristband and interacting with the system by placing their wrist between the two horn antennas. In this case, the subjects have been asked to keep their hands in bound conditions, in order to replicate the favorable conditions examined in Section V-B.

The mean EER achievable when exploiting the amplitudes of the considered scattering parameters is within the interval 5.2% ± 0.4%, with a considerable gain (a relative improvement in the order of 20%) with respect to the one obtained without the proposed MTS wristband, which is equal to 6.5% ± 0.4%, as shown in Table IV.

Fig. 6 shows the performance achievable when focusing on specific subbands, each with a width of 300 MHz, when selecting the components of the employed representations $\boldsymbol{s}$ using only the amplitude of the measured scattering parameters over the selected ranges ($F = 45$). The reported EERs are consistently better over the considered frequency range when the proposed MTS wristband is worn.

VI. CONCLUSION

In this article, the feasibility of designing a contactless biometric recognition system based on the EM interaction of a user's hand with the field radiated by two MW antennas working in the X-band has been investigated.

The results obtained from tests performed on 43 subjects show the existence of discriminative characteristics within the scattering parameters measured during the interaction, with the proposed system representing an interesting alternative to the currently deployed biometric system. In addition, this approach can be considered to complement existing systems, thus obtaining multibiometric solutions and increasing the overall system security, especially due to its effectiveness in guaranteeing robustness against possible spoofing attacks.

In order to improve the recognition performance achievable through the proposed approach, an MTS wristband has been designed with the aim of emphasizing the subject-specific EM characteristics of a user's hand. The results obtained when the involved users wear the fabricated MTS wristband confirm its effectiveness in enhancing the attainable recognition rates, thus allowing to exploit the considered EM interaction to implement a robust stand-alone biometric recognition system.

Future studies along this line of research may concern the use of different signal processing approaches for the considered scattering parameters, and the exploitation of better performing classifiers, for instance, investigating solutions based on neural networks. Furthermore, to evaluate the applicability of the proposed system to real-world scenarios, it would be advisable to conduct longitudinal studies aimed at verifying the permanence of the exploited discriminative characteristics over long time intervals [51] and to design template update strategies aimed at handling the variations in the identifiers of each user following each recognition attempt.

REFERENCES

[1] A. K. Jain, K. Nandakumar, and A. Ross, "50 years of biometric research: Accomplishments, challenges, and opportunities," *Pattern Recognit. Lett.*, vol. 79, pp. 80–105, Aug. 2016.
[2] V. Nagaraju and L. Fiondella, "A survey of homeland security biometrics and forensics research," in *Proc. IEEE Symp. Technol. Homeland Secur. (HST)*, May 2016, pp. 1–7.
[3] Z. Rui and Z. Yan, "A survey on biometric authentication: Toward secure and privacy-preserving identification," *IEEE Access*, vol. 7, pp. 5994–6009, 2019.
[4] S. Marcel, J. Fierrez, and N. Evans, *Handbook of Biometric Anti-Spoofing: Presentation Attack Detection and Vulnerability Assessment*. Singapore: Springer, 2023.
[5] K. Kavita, G. S. Walia, and R. Rohilla, "A contemporary survey of unimodal liveness detection techniques: Challenges & opportunities," in *Proc. 3rd Int. Conf. Intell. Sustain. Syst. (ICISS)*, Dec. 2020, pp. 848–855.
[6] A. Nait-Ali, *Hidden Biometrics*. Singapore: Springer, 2019.
[7] A. Uhl, C. Busch, S. Marcel, and R. Veldhuis, *Handbook of Vascular Biometrics*. Berlin, Germany: Springer, 2020.
[8] A. H. Mohsin et al., "Finger vein biometrics: Taxonomy analysis, open challenges, future directions, and recommended solution for decentralised network architectures," *IEEE Access*, vol. 8, pp. 9821–9845, 2020.
[9] G. Melia, "Electromagnetic absorption by the human body from 1–15 GHz," Ph.D. dissertation, Dept. Electron., Univ. York, York, U.K., 2013.
[10] J. F. Zhao, X. M. Chen, B. D. Liang, and Q. X. Chen, "A review on human body communication: Signal propagation model, communication performance, and experimental issues," *Wireless Commun. Mobile Comput.*, vol. 2017, Oct. 2017, Art. no. 5842310.

[11] D. Rissacher and D. Galy, "Cardiac radar for biometric identification using nearest neighbour of continuous wavelet transform peaks," in *Proc. IEEE Int. Conf. Identity, Secur. Behav. Anal. (ISBA)*, Mar. 2015, pp. 1–6.
[12] T. Okano, S. Izumi, H. Kawaguchi, and M. Yoshimoto, "Non-contact biometric identification and authentication using microwave Doppler sensor," in *Proc. IEEE Biomed. Circuits Syst. Conf. (BioCAS)*, Turin, Italy, Oct. 2017, pp. 1–4.
[13] S. M. M. Islam and V. M. Lubecke, "BreathID: Radar's new role in biometrics," *IEEE Aerosp. Electron. Syst. Mag.*, vol. 36, no. 12, pp. 16–23, Dec. 2021.
[14] A. Alkasimi et al., "Dual-biometric human identification using radar deep transfer learning," *Sensors*, vol. 22, no. 15, p. 5782, Aug. 2022.
[15] Q. Xu, Y. Chen, B. Wang, and K. J. R. Liu, "Radio biometrics: Human recognition through a wall," *IEEE Trans. Inf. Forensics Security*, vol. 12, no. 5, pp. 1141–1155, May 2017.
[16] F. Wang, J. Han, F. Lin, and K. Ren, "WiPIN: Operation-free passive person identification using Wi-Fi signals," in *Proc. IEEE Global Commun. Conf. (GLOBECOM)*, Dec. 2019, pp. 1–6.
[17] J. Liu, Y. Chen, Y. Dong, Y. Wang, T. Zhao, and Y.-D. Yao, "Continuous user verification via respiratory biometrics," in *Proc. IEEE INFOCOM Conf. Comput. Commun.*, Toronto, ON, Canada, Jul. 2020, pp. 1–10.
[18] P. Huang, D. Zhang, R. Geng, and Y. Chen, "Continuous user authentication using WiFi," in *Proc. Asia–Pacific Signal Inf. Process. Assoc. Annu. Summit Conf. (APSIPA ASC)*, Nov. 2022, pp. 2083–2088.
[19] A. Pokkunuru, K. Jakkala, A. Bhuyan, P. Wang, and Z. Sun, "NeuralWave: Gait-based user identification through commodity WiFi and deep learning," in *Proc. IECON 44th Annu. Conf. IEEE Ind. Electron. Soc.*, Washington, DC, USA, Oct. 2018, pp. 758–765.
[20] Y. Cao, Z. Zhou, C. Zhu, P. Duan, X. Chen, and J. Li, "A lightweight deep learning algorithm for WiFi-based identity recognition," *IEEE Internet Things J.*, vol. 8, no. 24, pp. 17449–17459, Dec. 2021.
[21] S. Liu, Y. Chen, H. Wang, H. Liang, and L. Chen, "A low-calculation contactless continuous authentication based on postural transition," *IEEE Trans. Inf. Forensics Security*, vol. 17, pp. 3077–3090, 2022.
[22] S. Yang, Y. Wang, X. Yu, Y. Gu, and F. Ren, "User authentication leveraging behavioral information using commodity WiFi devices," in *Proc. IEEE/CIC Int. Conf. Commun. China (ICCC)*, Chongqing, China, Aug. 2020, pp. 530–535.
[23] C. Zhao et al., "RF-Mehndi: A fingertip profiled RF identifier," in *Proc. IEEE Conf. Comput. Commun.*, Paris, France, Apr. 2019, pp. 1513–1521.
[24] J. Liu, X. Zou, F. Lin, J. Han, X. Xu, and K. Ren, "Hand-key: Leveraging multiple hand biometrics for attack-resilient user authentication using COTS RFID," in *Proc. IEEE 41st Int. Conf. Distrib. Comput. Syst. (ICDCS)*, Jul. 2021, pp. 1042–1052.
[25] W. Saadat, S. A. Raurale, G. A. Conway, and J. McAllister, "Physical layer biometrics using antennas for secure wearable wireless communication," *IEEE Trans. Antennas Propag.*, vol. 67, no. 4, pp. 2677–2686, Apr. 2019.
[26] W. Saadat, S. A. Raurale, G. A. Conway, and J. McAllister, "Wearable antennas for human identification at 2.45 GHz," *IEEE Trans. Antennas Propag.*, vol. 70, no. 1, pp. 17–26, Jan. 2022.
[27] K. Diederichs, A. Qiu, and G. Shaker, "Wireless biometric individual identification utilizing millimeter waves," *IEEE Sensors Lett.*, vol. 1, no. 1, pp. 1–4, Feb. 2017.
[28] K. Assaleh, N. Qaddoumi, T. Shanableh, and M. Adel, "A novel biometric via hand structure using near-field microwave imaging," in *Proc. IEEE Int. Conf. Autom. Face Gesture Recognit. (FG)*, Santa Barbara, CA, USA, Mar. 2011, pp. 167–172.
[29] E. Hof, A. Sanderovich, M. Salama, and E. Hemo, "Face verification using 802.11 waveforms," in *Proc. IEEE Int. Conf. Human-Machine Syst. (ICHMS)*, Rome, Italy, Sep. 2020, pp. 1–4.
[30] S. R. Heyes and R. M. Edwards, "Recognising people using smart phone antennas: A fuzzy biometric," in *Proc. Loughborough Antennas Propag. Conf. (LAPC)*, 2017, pp. 1–6.
[31] E. Maiorana, D. Ramaccia, L. Stefanini, A. Toscano, F. Bilotti, and P. Campisi, "Biometric recognition using microwave reflection spectroscopy," in *Proc. 24th Int. Microw. Radar Conf. (MIKON)*, Gdansk, Poland, Sep. 2022, pp. 1–5.
[32] D. Pozar, *Microwave Engineering*, 4th ed. Hoboken, NJ, USA: Wiley, 2011.
[33] Y. Lin Wang, Z. Yu Chen, and N. Hua Zhu, "Choice of calibration equations of the TSM method," in *Proc. 3rd Int. Conf. Microw. Millim. Wave Technol.*, Beijing, China, 2002, pp. 150–153.
[34] J. Wang, C. Lu, M. Wang, P. Li, S. Yan, and X. Hu, "Robust face recognition via adaptive sparse representation," *IEEE Trans. Cybern.*, vol. 44, no. 12, pp. 2368–2378, Dec. 2014.
[35] C. L. Holloway, E. F. Kuester, J. A. Gordon, J. O'Hara, J. Booth, and D. R. Smith, "An overview of the theory and applications of metasurfaces: The two-dimensional equivalents of metamaterials," *IEEE Antennas Propag. Mag.*, vol. 54, no. 2, pp. 10–35, Apr. 2012.
[36] S. B. Glybovski, S. A. Tretyakov, P. A. Belov, Y. S. Kivshar, and C. R. Simovski, "Metasurfaces: From microwaves to visible," *Phys. Rep.*, vol. 634, pp. 1–72, May 2016.
[37] L. Stefanini et al., "Multibeam scanning antenna system based on beamforming metasurface for fast 5G NR initial access," *IEEE Access*, vol. 10, pp. 65982–65995, 2022.
[38] D. Ramaccia, A. Toscano, A. Colasante, G. Bellaveglia, and R. Lo Forti, "Inductive tri-band double element FSS for space applications," *Prog. Electromagn. Res. C*, vol. 18, pp. 87–101, 2011.
[39] M. Barbuto et al., "Metasurfaces 3.0: A new paradigm for enabling smart electromagnetic environments," *IEEE Trans. Antennas Propag.*, vol. 70, no. 10, pp. 8883–8897, Oct. 2022.
[40] D. Ramaccia, D. L. Sounas, A. Alu, A. Toscano, and F. Bilotti, "Metasurface-based radar jammers and deceptors implemented through time-varying metasurfaces," in *Proc. 14th Eur. Conf. Antennas Propag. (EuCAP)*, Copenhagen, Denmark, Mar. 2020, pp. 1–2.
[41] A. Li, S. Singh, and D. Sievenpiper, "Metasurfaces and their applications," *Nanophotonics*, vol. 7, no. 6, pp. 989–1011, Jun. 2018.
[42] D. Ramaccia, A. Toscano, and F. Bilotti, "Scattering and absorption from super-spherical nanoparticles: Analysis and design for transparent displays [invited]," *J. Opt. Soc. Amer. B, Opt. Phys.*, vol. 34, no. 7, pp. 62–67, 2017.
[43] D. Ramaccia, S. Arcieri, A. Toscano, and F. Bilotti, "Core-shell super-spherical nanoparticles for LSPR-based sensing platforms," *IEEE J. Sel. Topics Quantum Electron.*, vol. 23, no. 2, pp. 380–387, Mar. 2017.
[44] F. Bilotti, A. Toscano, and L. Vegni, "Design of spiral and multiple split-ring resonators for the realization of miniaturized metamaterial samples," *IEEE Trans. Antennas Propag.*, vol. 55, no. 8, pp. 2258–2267, Aug. 2007.
[45] A. M. Siddiky, M. R. I. Faruque, M. T. Islam, and S. Abdullah, "A multi-split based square split ring resonator for multiband satellite applications with high effective medium ratio," *Results Phys.*, vol. 22, Mar. 2021, Art. no. 103865.
[46] Dielectric Properties. *IT'IS Foundation (No Date)*. Accessed: Mar. 17, 2023. [Online]. Available: https://itis.swiss/virtual-population/tissue-properties/database/dielectric-properties/
[47] Y.-J. An, B.-H. Kim, G.-H. Yun, S.-W. Kim, S.-B. Hong, and J.-G. Yook, "Flexible non-constrained RF wrist pulse detection sensor based on array resonators," *IEEE Trans. Biomed. Circuits Syst.*, vol. 10, no. 2, pp. 300–308, Apr. 2016.
[48] B.-H. Kim et al., "A proximity coupling RF sensor for wrist pulse detection based on injection-locked PLL," *IEEE Trans. Microw. Theory Techn.*, vol. 64, no. 5, pp. 1667–1676, May 2016.
[49] *3DS Simulia CST Studio Suite*. Accessed: Mar. 17, 2023. [Online]. Available: https://www.3ds.com/products-services/simulia/
[50] *LPKF ProtoLaser H4*. Accessed: Mar. 17, 2023. [Online]. Available: https://www.lpkf.com/en/industries-technologies/research-in-house-pcb-prototyping/products/lpkf-protolaser-h4
[51] M. Fairhurst, *Age Factors in Biometric Processing*. London, U.K.: IET, 2013.

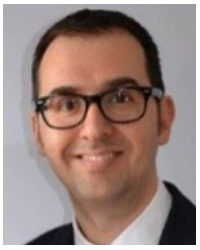

Emanuele Maiorana (Senior Member, IEEE) received the Ph.D. degree in biomedical, electromagnetism, and telecommunication engineering from Roma Tre University, Rome, Italy, in 2009, with European Doctorate Label.

He is currently an Assistant Professor with the Department of Industrial, Electronic and Mechanical Engineering, Roma Tre University. His research interests are in the area of digital signal and image processing, with a specific emphasis on biometric recognition.

Dr. Maiorana was a recipient of the Lockheed Martin Best Paper Award for the Poster Track at the IEEE Biometric Symposium 2007, the Honeywell Student Best Paper Award at the IEEE Biometrics: Theory, Applications and Systems Conference 2008, and the Best Paper Award at the 11th International Conference on Pattern Recognition Applications and Methods (ICPRAM) 2022. He was the General Chair of the 9th IEEE International Workshop on Biometrics and Forensics (IWBF) 2021. He is an Associate Editor of the IEEE TRANSACTIONS ON INFORMATION FORENSICS AND SECURITY.

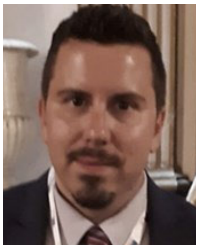

Davide Ramaccia (Senior Member, IEEE) received the B.S. and M.S. degrees (summa cum laude) in electronic and ICT engineering and the Ph.D. degree in electronic engineering from Rome Tre University, Rome, Italy, in 2007, 2009, and 2013, respectively.

He was with the Department of Engineering, from 2013 to 2021, and has been with the Department of Industrial, Electronic, and Mechanical Engineering, since 2021, with Roma Tre University. He has coauthored more than 100 articles in international journals, conference proceedings, and book chapters and holds one patent. His main research interests include the modeling and design of (space–)time-varying metamaterials and metasurfaces and their applications to microwave components and antennas, and the analysis of anomalous scattering effects in temporal metamaterials.

Dr. Ramaccia has been serving as a member for the Steering Committee of the International Congress on Advanced Electromagnetic Materials in Microwaves and Optics—Metamaterials Congress since 2015. In 2022, he was appointed as a member of the IEEE APS Award Committee by the IEEE APS Society. Since 2021, he has been serving as a member for the Technical Program Committee of the International Congress on Laser Science and Photonics Applications—CLEO (Eds., 2022 and 2023). He has been serving the scientific community, by playing roles in the management of scientific societies, on the editorial board of international journals, and in the organization of conferences and courses. He was a recipient of a number of awards and recognitions, including the Electromagnetics Academy Young Scientist Award in 2019, seven Outstanding Reviewer Awards by the IEEE TRANSACTIONS ON ANTENNAS AND PROPAGATION from 2013 to 2021, the IET prizes for the Best Poster on Microwave Metamaterials in 2013, and the IET Award for the Best Poster on the Metamaterial Application in antenna field in 2011. He is currently the General Secretary of the Virtual Institute for Artificial Electromagnetic Materials and Metamaterials (METAMORPHOSE VI, the International Metamaterials Society) and has been an Elected Member of the Board of Directors of the same association for three consecutive terms since 2014. He was also a Guest Co-Editor of three special issues on metamaterials and metasurfaces and a Lead Guest-Editor for the Special Cluster on Metadome for Antenna Systems for IEEE ANTENNAS AND WIRELESS PROPAGATION LETTERS in 2022. He has been the General Chair and a Local Organizer of the 39th and 42nd EUPROMETA Doctoral School on Metamaterials held in Rome, in 2019 and 2021, respectively. He has been a Technical Program Coordinator (Track "Electromagnetics and Materials") for the 2016 IEEE Antennas and Propagation Symposium. He was elected as the Secretary of the Project Management Board of the H2020 CSA Project Nanoarchitectronics from 2017 to 2018. He has been serving as an Associate Editor for IEEE ACCESS since 2019, a Scientific Moderator for IEEE Techrxiv since 2019, and a technical reviewer for the major international journals related to electromagnetic field theory and metamaterials.

Luca Stefanini (Graduate Student Member, IEEE) was born in Rome, Italy, in 1996. He received the bachelor's degree in electronic engineering and the master's degree in electronic engineering for industry and innovation from Roma Tre University, Rome, Italy, in 2018 and 2021, respectively, where he is currently pursuing the Ph.D. degree in applied electronics.

His research interests include metasurface and metamaterial field, spanning from metasurface for antenna systems to temporal metamaterials.

Alessandro Toscano (Senior Member, IEEE) was born in Capua, Italy, in 1964. He received the degree in electronic engineering and the Ph.D. degree from the Sapienza University of Rome, Rome, Italy, in 1988 and 1993, respectively.

Since 2011, he has been a Full Professor of electromagnetic fields with the Engineering Department, Roma Tre University, Rome. He carries out intense academic and scientific activity, both nationally and internationally. He has held numerous invited lectures at universities, public and private research institutions, and national and international companies about artificial electromagnetic materials, metamaterials, and their applications. He actively participated in founding the International Association on Metamaterials Virtual Institute for advanced electromagnetic materials—METAMORPHOSE, VI. He coordinates and participates in several research projects and contracts funded by national and international public and private research institutions and industries. He has authored or coauthored over 150 publications in international journals indexed ISI or Scopus; of these on a worldwide scale, five are in the first 0.1 percentile, ten in the first 1 percentile, and 25 in the first 5 percentile in terms of the number of quotations and journal quality.He is currently a member of the Board of Director of Radiolabs and Labchain (non-for-profit Research Consortia), and the Scientific Council of CIRIAF (Interuniversity Research Center on Pollution and the Environment). His scientific research has as ultimate objective of conceiving, designing, and manufacturing of innovative electromagnetic components with a high technological content that shows enhanced performance compared with those obtained with traditional technologies and that respond to the need for environment and human health protection. His research activities are focused on three fields: metamaterials and unconventional materials, in collaboration with Professor A. Alù's group at The University of Texas at Austin, Austin, TX, USA, research and development of electromagnetic cloaking devices and their applications (First Place Winner of the Leonardo Group Innovation Award for the research project entitled: "Metamaterials and electromagnetic invisibility"), and the research and manufacturing of innovative antenna systems and miniaturized components (First Place Winner of the Leonardo Group Innovation Award for the research project entitled: "Use of metamaterials for miniaturization of components"—MiniMETRIS).

Dr. Toscano was a member of the Roma Tre University Academic Senate from 2013 to 2018. He was a member of the National Commission which enables National Scientific Qualifications to a full professor and an associate professor in the tender sector 09/F1—Electromagnetic fields from 2016 to 2018. From 2018 to 2022, he has been a Vice-Rector for Innovation and Technology Transfer and member of the Steering Committee of the National Competence Center on Cyber 4.0. He is currently a member of the Board of Director of Radiolabs and Labchain (non-for-profit Research Consortia), and the Scientific Council of CIRIAF (Interuniversity Research Center on Pollution and the Environment). In addition to his commitment in organizing scientific events, he also carries out an intense editorial activity as a member of the review committees of major international journals and conferences in the field of applied electromagnetics.

Filiberto Bilotti (Fellow, IEEE) received the Laurea and Ph.D. degrees in electronic engineering from Roma Tre University, Rome, Italy, in 1998 and 2002, respectively.

Since 2002, he has been a Faculty Member at Roma Tre University, serving as a Full Professor of electromagnetic field theory at the Department of Industrial, Electronic, and Mechanical Engineering. Since 2012, he has been the Director of the Antennas and Metamaterials Research Laboratory. His main research interests include the analysis and design of microwave antennas and arrays and analytical modeling of artificial electromagnetic materials, metamaterials, and metasurfaces, including their applications at both microwave and optical frequencies. The research activities developed in the last 20 years have resulted in more than 620 papers in international journals, conference proceedings, book chapters, and three patents. In the last ten years, his main research interests include the development of intelligent nodes for smart electromagnetic environments; the modeling, design, implementation, and application of reconfigurable intelligent metasurfaces; the modeling and applications of (space and) time-varying metasurfaces; the topological-based design of antennas supporting structured field; the analysis and design of cloaking metasurfaces for antenna systems; the concept of meta-gratings and related applications in optics and at microwaves; and the modeling and applications of optical metasurfaces.

Prof. Bilotti was a recipient of a number of awards and recognitions, including the elevation to the IEEE Fellow Grade for contributions to metamaterials for electromagnetic and antenna applications in 2017; the Chen-To-Tai Distinguished Educator Award of the IEEE Antennas and Propagation Society in 2023; the Outstanding Associate Editor for the IEEE TRANSACTIONS ON ANTENNAS AND PROPAGATION in 2016 and 2023; the NATO SET Panel Excellence Award in 2016; the Finmeccanica Group Innovation Prize in 2014; the Finmeccanica Corporate Innovation Prize in 2014; the IET Best Poster Paper Award (Metamaterials 2013 and Metamaterials 2011); and the Raj Mittra Travel Grant Senior Researcher Award in 2007. He has been serving the scientific community, by playing leading roles in the management of scientific societies, on the editorial board of international journals, and in the organization of conferences and courses. In particular, he was a Founding Member of the Virtual Institute for Artificial Electromagnetic Materials and Metamaterials—METAMORPHOSE VI in 2007. He was elected as a member of the Board of Directors of the same society for two terms from 2007 to 2013 and the President for two terms from 2013 to 2019. He has been serving the METAMORPHOSE VI as the Vice President and has been the Executive Director since 2019. He served/serves as a member of the Editorial Board for the International Journal of RF and Microwave Computer-Aided Engineering from 2009 to 2015, Nature Scientific Reports from 2013 to 2016, and EPJ Applied Metamaterials since 2013. He was also a Guest Editor of six special issues in international journals and served as an Associate Editor for the Metamaterials Journal from 2007 to 2013 and the IEEE TRANSACTIONS ON ANTENNAS AND PROPAGATION from 2013 to 2017 and 2022. In 2007, he organized the inaugural edition of the International Congress on Advanced Electromagnetic Materials in Microwaves and Optics—Metamaterials Congress, served as the Chair for the Steering Committee of the same conference for eight editions from 2008 to 2014 and in 2019; and was elected as the General Chair of the Metamaterials Congress from 2015 to 2018. He was also the General Chair of the Second International Workshop on Metamaterials-by-Design Theory, Methods, and Applications to Communications and Sensing in 2016 and has been serving as the Chair or a member for the technical program, steering, and organizing committee of the main national and international conferences in the field of applied electromagnetics.

Patrizio Campisi (Fellow, IEEE) received the Ph.D. degree in electrical engineering from Roma Tre University, Rome, Italy.

He is currently a Full Professor with the Department of Industrial, Electronics and Mechanical Engineering, Roma Tre University. His current research interests are in the area of biometrics and secure multimedia communications.

Dr. Campisi is the Vice President of Publications for the IEEE Biometrics Council. He was the IEEE SPS Director Student Services from 2015 to 2017 and the Chair of the IEEE Technical Committee on Information Forensics and Security from 2017 to 2018. He was the General Chair of the 26th European Signal Processing Conference EUSIPCO 2018, Italy, the 7th IEEE Workshop on Information Forensics and Security (WIFS) 2015, Italy, and the 12th ACM Workshop on Multimedia and Security 2010, Italy. He was an Associate Editor and a Senior Associate Editor of the IEEE SIGNAL PROCESSING LETTERS and an Associate Editor of the IEEE TRANSACTIONS ON INFORMATION FORENSICS AND SECURITY. He was the Editor-in-Chief of the IEEE TRANSACTIONS ON INFORMATION FORENSICS AND SECURITY.

Open Access funding provided by 'Università degli Studi Roma Tre' within the CRUI CARE Agreement